

Crystallization Behavior and Isothermal Crystallization Kinetics of PLLA Blended with Ionic Liquid, 1-Butyl-3-methylimidazolium Dibutylphosphate

Taiyan Wei,^{1,2} Sujuan Pang,^{1,2} Nai Xu,^{1,2} Lisha Pan,^{1,2} Zhengqing Zhang,^{1,2} Ruizhang Xu,^{1,2} Nansong Ma,^{1,2} Qiang Lin³

¹College of Materials and Chemical Engineering, Hainan University, Hainan, Haikou 570228, China

²Hainan Provincial Fine Chemical Engineering Research Center, Hainan University, Hainan, Haikou 570228, China

³College of Chemistry and Chemical Engineering, Hainan Normal University, Hainan, Haikou 571158, China

Correspondence to: N. Xu (E-mail: xunai1978@gmail.com)

ABSTRACT: The crystallization behavior and isothermal crystallization kinetics of neat poly(L-lactic acid) (PLLA) and PLLA blended with ionic liquid (IL), 1-butyl-3-methylimidazolium dibutylphosphate, were researched by differential scanning calorimetry (DSC), polarizing optical microscopy (POM), and wide angle X-ray diffraction (WXR). Similar to the non-isothermal crystallization behavior of neat PLLA, when PLLA melt was cooled from 200 to 20°C at a cooling rate of 10°C min⁻¹, no crystallization peak was detected yet with the incorporation of IL. However, the glass transition temperature and cold crystallization temperature of PLLA gradually decreased with the increase of IL content. It can be attributed to the significant plasticizing effect of IL, which improved the chain mobility and cold crystallization ability of PLLA. Isothermal crystallization kinetics was also analyzed by DSC and described by Avrami equation. For neat PLLA and IL/PLLA blends, the Avrami exponent *n* was almost in the range of 2.5–3.0. It is found that *t*_{1/2} reduced largely, and the crystallization rate constant *k* increased exponentially with the incorporation of IL. These results show that the IL could accelerate the overall crystallization rate of PLLA due to its plasticizing effect. In addition, the dependences of crystallization rate on crystallization temperature and IL content were discussed in detail according to the results obtained by DSC and POM measurements. It was verified by WXR that the addition of IL could not change the crystal structure of PLLA matrix. All samples isothermally crystallized at 100°C formed the α -form crystal. © 2014 Wiley Periodicals, Inc. *J. Appl. Polym. Sci.* **2015**, *132*, 41308.

KEYWORDS: biodegradable; crystallization; differential scanning calorimetry (DSC); ionic liquids; kinetics

Received 19 November 2013; accepted 23 July 2014

DOI: 10.1002/app.41308

INTRODUCTION

Ionic liquids (ILs) are low melting point salts melt ($T_m < 100^\circ\text{C}$) and typically consist of a bulky organic cation and an anion. Because ILs have enormous potential, such as low toxicity, negligible vapor pressure, low inflammability, non-explosive, high electric conductivity, and thermal stability, the ILs are considered as green alternatives to volatile organic compounds in organic synthesis, catalysis, chromatography, extraction, electroanalytical chemistry, sensing, spectrometry, etc.^{1–4}

Moreover, ILs have been proved to work as plasticizers, lubricants, and even retardants for universal polymers, including of PMMA,⁵ PVC,^{6,7} PC,⁸ and PU.⁹

Poly(L-lactic acid) (PLLA) is a novel kind of green biodegradable and linear aliphatic thermoplastics, which is produced from renewable resources, such as corn and wheat straw. Since

PLLA is compostable and derived from sustainable resources, it has been viewed as a promising material to reduce the societal solid waste disposal problem. Its low toxicity, along with its environmentally benign characteristics, has made PLLA an ideal material for consumer products in the 21st century.¹⁰

However, the final products of PLLA obtained by the traditional processing technology usually are low of crystallinity even amorphous owing to the slow crystallization rate of PLLA. Due to its low crystallinity and glass transition temperature (T_g) of around 50–60°C, the mechanical properties of neat PLLA is unsatisfied, such as brittleness, poor thermal-dimensional stability, which restrict its development and practical application.¹⁰

Introduction of plasticizers is an important method to improve the toughness of PLLA. Varying types of plasticizers such as citrate esters, triacetine, poly(ethylene glycol), poly(propylene glycol), oligomeric lactic acid, glycerol, tributyl

citrate, tributyl citrate oligomers, glucosemono esters, and partial fatty acid ester were found to be efficient plasticizers for PLLA.^{11–16}

Recently, research efforts have shown that ILs can also be used as efficient plasticizers or lubricants for poly(lactic acid).^{17–19}

In Bor-Kuan Chen's study,¹⁷ ILs/PLLA blends were prepared by solution casting method, and four ILs: 1-methyl-3-pentylimidazolium tetrafluoroborate ([MPI][BF₄]), 1-methyl-3-pentylimidazolium hexafluorophosphate ([MPI][PF₆]), 1-methyl-3-pentylimidazolium bis(trifluoromethanesulfonyl) imide ([MPI][TFSI]), and 1,2-dimethyl-3-pentyl imidazolium bis(trifluoromethanesulfonyl) imide ([DMPI][TFSI]) were chosen to enhance the ductility of PLLA. The obtained ILs/PLLA samples had very high elongation at break (increased by 10–25 times when compared with neat PLLA). Moreover, TGA data demonstrated higher thermal stability of ILs/PLLA samples than neat PLLA, which can be attributed to the high temperature stability of ILs. The sequence of the effects on the thermal property of imidazolium ILs modified PLLA samples was [PF₆] > [BF₄] > [TFSI].

Park and Xanthos¹⁸ reported that two phosphonium cation-based ILs with different anions appeared to be potential plasticizers and/or lubricants for PLLA. Both ILs lowered the glass transition temperature of PLLA and modified its rheological characteristics as evidenced from reduced viscosities and apparent phase separation and lubrication. In their later research,¹⁹ two ILs with different anions (decanoate, tetrafluoroborate) but with the same phosphonium-based cation were evaluated as potential plasticizers and lubricants for PLLA. Both ILs at 5 wt % were well dispersible and partly miscible with PLLA as evidenced by scanning electron microscopy and glass transition temperature (T_g) characterization, as well as from solubility parameters calculations. However, phase separation in the PLLA system containing the IL with tetrafluoroborate anions was observed 1 year after melt processing. The effects of the IL containing the tetrafluoroborate anion were more pronounced on lubrication as evidenced by lower values of coefficient of friction that could also be correlated with lower contact angle; this IL could then be considered as a more effective plasticizer than the IL containing the decanoate anion based on reduced flexural modulus and brittleness as well as T_g suppression results.

It is well-known that the crystallization behavior, crystalline structure, and morphology of semicrystalline polymers play important roles in their physical properties. To the best of our knowledge, although a couple of papers focusing on the plasticizing/lubricating effects of ILs on PLLA have been reported, the crystallization behavior, especially isothermal crystallization behavior of PLLA in the presence of IL has not been researched sufficiently. In this article, crystallization behavior and crystal structure of IL/PLLA blends with various IL contents were investigated using differential scanning calorimetry (DSC), polarizing optical microscopy (POM), and wide angle X-ray diffraction (WAXRD). Furthermore, to better understand the effect of IL on the crystallization behavior of PLLA, isothermal crystallization kinetics was analyzed according to Avrami equation.

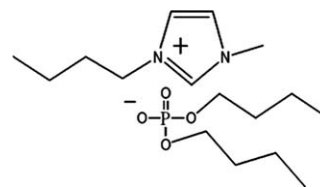


Figure 1. Structures of [BMIM][(C₄H₉O)₂PO₂].

EXPERIMENTAL

Materials

PLLA supplied by NatureWorks LLC was a semicrystalline grade (4032D) comprising around 2% D-LA. Butyl-3-methylimidazolium dibutylphosphate, [BMIM][(C₄H₉O)₂PO₂] was purchased from Cheng Jie Chemical, Shanghai, China. Structures of [BMIM][(C₄H₉O)₂PO₂] are shown in Figure 1.

Sample Preparation

The PLLA pellets and IL were dried at 60°C in a vacuum oven for 12 h prior to processing. Varying amounts of IL (1, 3, 6, and 9, in wt %) were mixed with PLLA melt at 180°C for 5 min in an internal mixer (LH60, Shanghai Kechuang Plastic Machinery Factory, China) with a screw speed of 60 rpm.

To make sure neat PLLA undergoes the same processing and thermal history, neat PLLA was also processed at 180°C for 5 min in the internal mixer with a screw speed of 60 rpm.

Thermal Analysis

The crystallization and melting behavior of IL/PLLA blends were investigated using a differential scanning calorimeter (Q100, TA instrument). Calibration was performed using pure indium at a heating rate of 10°C min⁻¹. All DSC measurements were conducted under a nitrogen atmosphere.

Before the start of a cycle, each sample (around 5 mg) was first heated to 200°C at a rate of 50°C min⁻¹ and held at the same temperature for 4 min to eliminate prior thermal history. And then, the melt was cooled down to 20°C from 200°C at a rate of -10°C min⁻¹. The non-isothermal crystallization behavior of IL/PLLA sample was recorded in the first cooling scan. After the cooling, the sample was heated to 200°C at a rate of 10°C min⁻¹ to record its cold crystallization and melting behavior. Glass transition temperature (T_g), cold crystallization temperature (T_{cc}), and melting temperature (T_m) were determined in the second heating scan.

For isothermal crystallization measurements, each sample (around 5 mg) was first heated to 200°C at a rate of 50°C min⁻¹ and held at the same temperature for 4 min to eliminate prior thermal history. And then, the melt was rapidly cooled down to a desired crystallization temperature, and the isothermal crystallization processes was recorded entirely until the exothermic enthalpy became completely invariant.

The crystallization kinetics of polymers under isothermal conditions for various modes of nucleation and growth can be well approximated by the well-known Avrami equation. The general form of the equation is given in eq. (1):^{20–22}

$$X(t) = 1 - \exp(-Kt^n) \quad (1)$$

where K is the Avrami rate constant containing the nucleation and the growth parameters, n is the Avrami exponent whose

value depends on the mechanism of nucleation and on the form of crystal growth, t denotes the real time of crystallization. $X(t)$ is related to the relative crystallinity at time t . $X(t)$ can be obtained from the ratio of the area of the exotherm up to time t divided by the total exotherm as follows:²⁰

$$X(t) = \frac{Q_t}{Q_\infty} = \frac{\int_0^t (dH/dt) dt}{\int_0^\infty (dH/dt) dt} \quad (2)$$

Where Q_t and Q_∞ are the heat generated at time t and infinite time, respectively, and dH/dt is the rate of heat evolution.

Taking its double logarithmic form, eq. (1) can be changed to

$$\log[-\ln(1-X(t))] = n \log t + \log K \quad (3)$$

From a graphic representation of $\log[-\ln(1-X(t))]$ versus t , the n (slope of the straight line) and K values (intersection with the Y-axis) can be calculated.

Differentiating eq. (1) twice, and when $d^2X(t)/dt^2 = 0$, the time at maximum heat flow t_{\max} can be expressed as:²²

$$t_{\max} = [(n-1)/nK]^{1/n} \quad (4)$$

And let eq. (1) equal to 0.5, the crystallization half-time ($t_{1/2}$) defined as the time to a relative crystallinity of 50% can be obtained:

$$t_{1/2} = (\ln 2/K)^{1/n} \quad (5)$$

POM Analysis

A Leica DMRX POM was applied to investigate the spherulitic growth and morphology of neat PLLA and IL/PLLA samples in different isothermal crystallization conditions.

Each sample was first inserted between two microscope coverslips and squeezed at 200°C to obtain a slice with a thickness of around 40 μm. Subsequently, the sandwiched slice was transferred as quickly as possible onto a hot stage to be isothermally crystallized at a given temperature for 3 min/or 30 min. Finally, the sample was removed from the hot stage and quenched to room temperature, and kept for POM observation.

WXR D Analysis

WXR D measurement was applied to investigate the effect of IL on crystalline structure of PLLA. The samples for WXR D measurements were prepared as follows: IL/PLLA samples were melted at 200°C and then pressed into films with a thickness of around 1 mm. The temperature was maintained at 200°C for 4 min to eliminate the thermal history. And then, the films were quickly transferred in a hot stage for isothermal crystallization at the given temperature of 100°C. When the crystallization time reached 20 min, the crystallized samples were quickly removed and quenched in ice water. WXR D patterns were recorded with a Bruker D8 ADVANCE XRD (Germany) system by using Cu Kα radiation in the scattering angle range of $2\theta = 3^\circ \sim 40^\circ$ with a scan speed of 2° min^{-1} at room temperature.

RESULTS AND DISCUSSION

Non-Isothermal DSC Analysis

The effect of IL on non-isothermal crystallization and melting behavior of PLLA was investigated. The DSC thermograms for PLLA and IL/PLLA samples cooled at $-10^\circ\text{C min}^{-1}$ and subse-

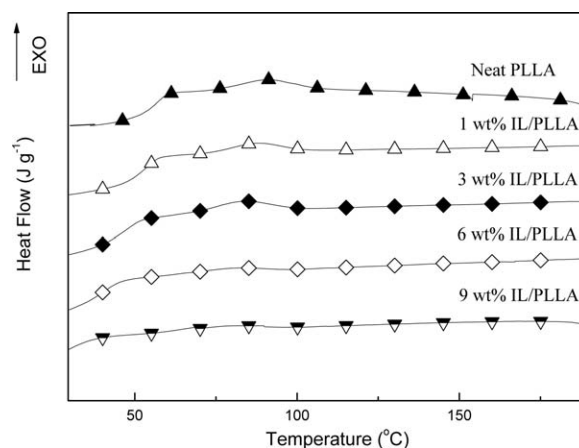


Figure 2. DSC trace of PLLA with various IL contents at a cooling rate of $-10^\circ\text{C min}^{-1}$.

quently heated at $10^\circ\text{C min}^{-1}$ are shown in Figures 2 and 3, respectively. The obtained DSC parameters are also given in Table I.

As expected, neat PLLA did not exhibit a crystallization peak upon cooling due to its weak melt-crystallization ability.^{10,13,23} Similar to neat PLLA, there was no obvious crystallization peak observed yet for the IL/PLLA samples, as shown in Figure 2. It indicates that the presence of IL could not significantly enhance the crystallization rate of PLLA when PLLA melt was cooled down at a cooling rate of $10^\circ\text{C min}^{-1}$.

However, as indicated in Figure 3, each PLLA sample shows a strong exothermic peak in the DSC thermogram obtained for subsequently heated at $10^\circ\text{C min}^{-1}$. These exothermic peaks are attributed to the cold crystallization of PLLA in amorphous solid state during the subsequent heating DSC scanning. The corresponding crystallization peak is known as the cold crystallization temperature (T_{cc}). Neat PLLA represented an exothermic peak at 103.4°C . However, in the case of the IL/PLLA samples, this peak shifted to lower temperature with the increase of IL content. When IL content increased to 9 wt %, T_{cc} of PLLA matrix decreased to 88.7°C from 103.4°C for neat PLLA. The improvement in cold crystallization ability of PLLA can be attributed to the plasticizing effect of IL which improved the mobility of PLLA segment.

To investigate the plasticizing effect of IL on PLLA, glass transition temperature (T_g) was measured and listed in Table I. As a general trend, the T_g of PLLA matrix obviously decreased to lower temperature with the increase of IL content. When IL content reached to 9 wt %, T_g of PLLA matrix decreased from 61.1°C for neat PLLA to 32.2°C . It suggests that the IL had an obvious plasticizing effect on PLLA, and enhanced the mobility of PLLA segment because the incorporation of IL resulted in larger free volume of PLLA segments than neat PLLA. The similar result also was reported by Park and Xanthos¹⁸ It was found that two phosphonium cation-based IL with different anions both lowered the T_g of PLLA matrix and appeared to be potential plasticizers and/or lubricants for PLLA.

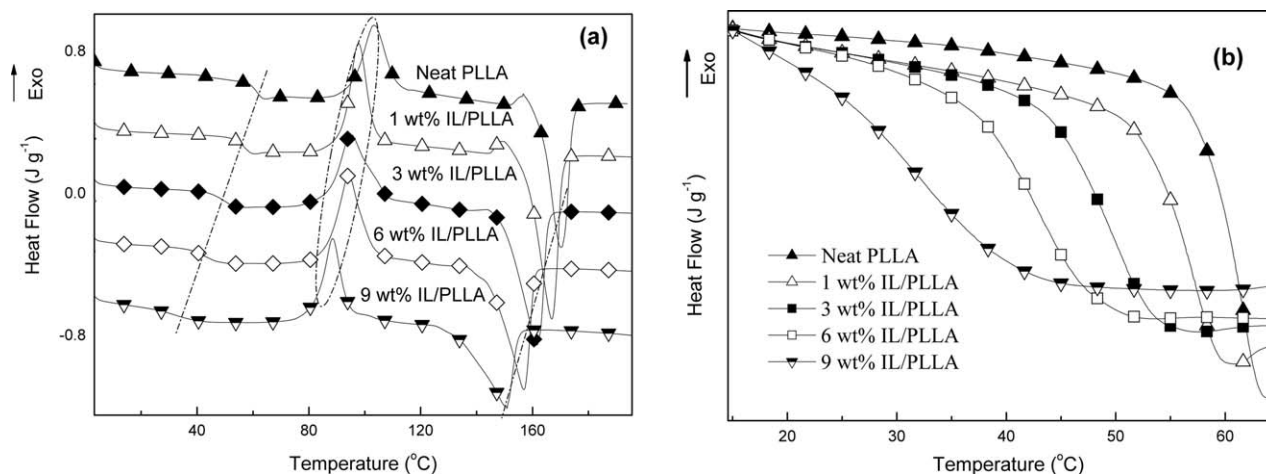


Figure 3. (a) DSC traces of heating process of neat PLLA and IL/PLLA samples at the rate of $10^{\circ}\text{C min}^{-1}$; (b) the detail with enlarged scale of (a).

Similar to T_g , T_m of PLLA matrix also gradually shifted down with increasing IL content as shown in Figure 3 and Table I. The depression of T_m can be attributed to the plasticizing effect of IL which enhances the chain mobility of PLLA. When the IL is introduced into PLLA matrix, the thermal mobility of PLLA chains is improved. As a result, these regular close-packed PLLA chains/segments in crystal could come into a state of random thermal motion in a relatively lower melting temperature.

ΔH_{cc} of the blends measured from the DSC thermograms are also listed in Table I. It was found that the value of ΔH_{cc} increased from 31.0 J g^{-1} for neat PLLA to 39.0 J g^{-1} for 3 wt % IL/PLLA blend, which was in agreement with the enhanced cold crystallization capacity mentioned above. However, when IL content exceeded 6 wt %, ΔH_{cc} began to decrease. It can be explained by the dilution effect of the amorphous phase of IL on the system.

Isothermal Crystallization Behavior and Kinetics

The isothermal crystallization behaviors of neat PLLA and IL/PLLA samples were investigated by DSC. Figure 4 shows the isothermal DSC thermograms of PLLA samples with different IL content at the crystallization temperature (T_c) of 90°C . It is found that the overall crystallization time to reach the maximum crystallinity for PLLA matrix reduced largely with the incorporation of IL. The overall crystallization time decreased from about 40 min for neat PLLA to about 2 min for 9 wt % IL/PLLA blend. The increase in crystallization rate of PLLA is attributed to the plasticizing effect of IL, resulting in the enhancement in chain mobility and crystallization ability of PLLA matrix.

Furthermore, to investigate the dependence of IL content and crystallization temperature on the isothermal crystallization behavior of PLLA, the molten PLLA samples with various IL content were quenched to a given crystallization temperature (T_c), respectively, and their exothermic peaks during the isothermal crystallization processes were recorded. According to eq. (1), $X(t)$ at different crystallization times can be calculated from the exothermic peaks. Plots of $X(t)$ versus crystallization time (t) for neat PLLA and IL/PLLA samples at different crystallization temperatures are showed in Figure 5. It seems that all the isotherms exhibit a sigmoid dependence with time. It is found that from Figure 5 that not only IL content but also crystallization temperature can significantly affect the overall crystallization time of PLLA.

The dependences of crystallization time on crystallization temperature and IL content will be further discussed in succession according to the calculations obtained from isothermal crystallization kinetics of PLLA samples.

Avrami equation [eq. (1)] was used to describe the isothermal crystallization kinetics of IL/PLLA samples. The plot of $\log[-\ln(1 - X(t))]$ versus $\log t$ according to eq. (1) are shown in Figure 6. It is found there is a linear relationship between $\log[-\ln(1 - X(t))]$ and $\log t$. Therefore, the linear portions of these plots were fitted for the isothermal crystallization kinetics analysis according to Avrami equation.

From Figure 6, Avrami parameters (n), and crystallization rate constant (k) for neat PLLA and IL/PLLA samples with various

Table I. Melting Endotherms Parameters of Neat PLLA and ILs/PLLA Samples

Sample	T_g ($^{\circ}\text{C}$)	T_{cc} ($^{\circ}\text{C}$)	T_m ($^{\circ}\text{C}$)	ΔH_{cc} (J g^{-1})	ΔH_m (J g^{-1})
Neat PLLA	61.1	103.4	170.2	31.0	36.2
1 wt % IL/PLLA	57.2	97.9	167.1	36.3	41.5
3 wt % IL/PLLA	49.7	95.4	161.2	39.0	42.3
6 wt % IL/PLLA	42.4	94.1	157.0	38.8	40.8
9 wt % IL/PLLA	32.2	88.7	151.1	35.1	35.6

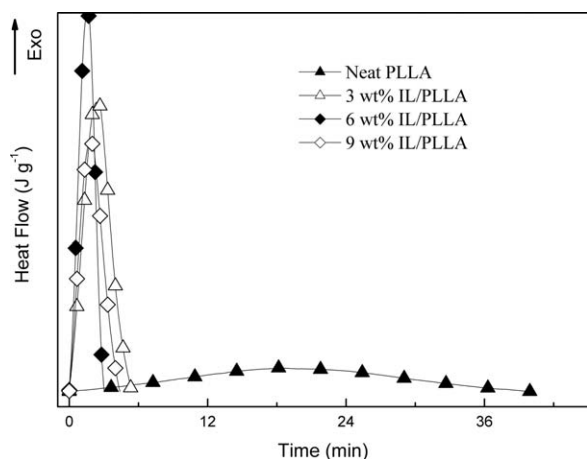


Figure 4. Isothermal crystallization process of PLLA and IL/PLLA samples at 90°C.

IL content were calculated according to eq. (1) and are listed in Table II. The crystallization half-time ($t_{1/2}$) were calculated by eq. (5) and are also listed in Table II.

As shown in Figure 6, all curves are divided into two sections: the primary crystallization stage and the secondary crystalliza-

tion stage. In the primary stage, the plots show a good linear relationship. As a result, the Avrami parameters can be calculated by fitting a line to these experimental data. At the secondary stage, the linear relationship shows a huge deviation. It is generally believed that the secondary crystallization is caused by the spherulite impingement in the later stage of crystallization process at longer crystallization time.

The values of n were almost in the range of 2.5–3.0 for neat PLLA at the different crystallization temperatures. It is an average value of various nucleation types, and the growth dimensions occurring simultaneous in the crystallization process. For neat PLLA without any heterogeneous nucleus, its nucleation type should predominantly be homogeneous nucleating and its growth dimension should be a two-dimensional growth.^{24,25} Compared with the values of n for neat PLLA, the values of n for IL/PLLA blends are still in the range of 2.5–3.0. For IL/PLLA samples, its nucleation type should mostly be heterogeneous nucleating and its growth dimension should mostly be two-dimensional space extension.

On the other hand, the values of crystallization rate constant k for IL/PLLA samples showed an exponential growth, and the values of crystallization half-time ($t_{1/2}$) decreased largely. The decrease of k and increase of $t_{1/2}$ meant that the overall

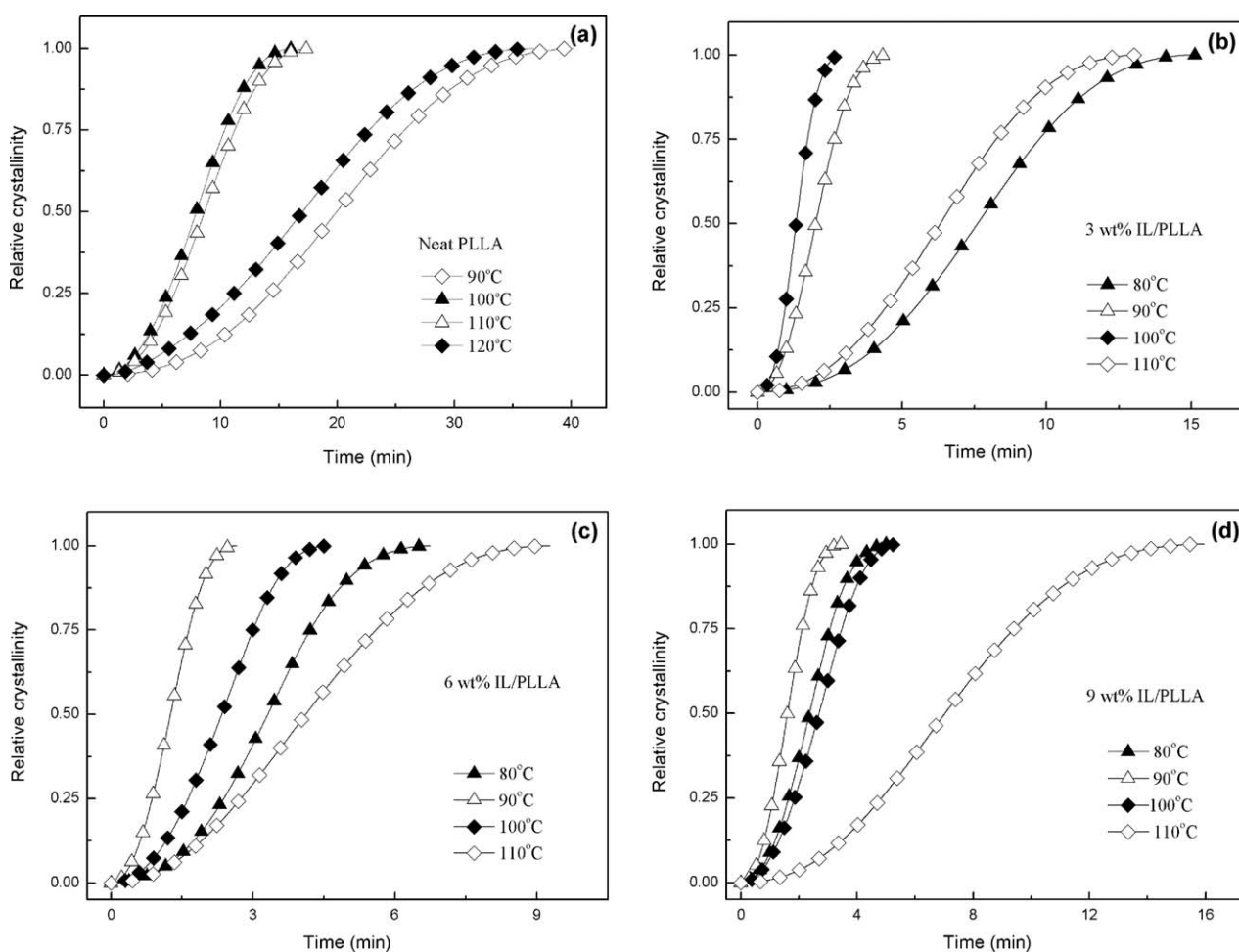


Figure 5. Plots of relative crystallinity as a function of crystallization time for (a) Neat PLLA; (b) 3 wt % IL/PLLA; (c) 6 wt % IL/PLLA; (d) 9 wt % IL/PLLA.

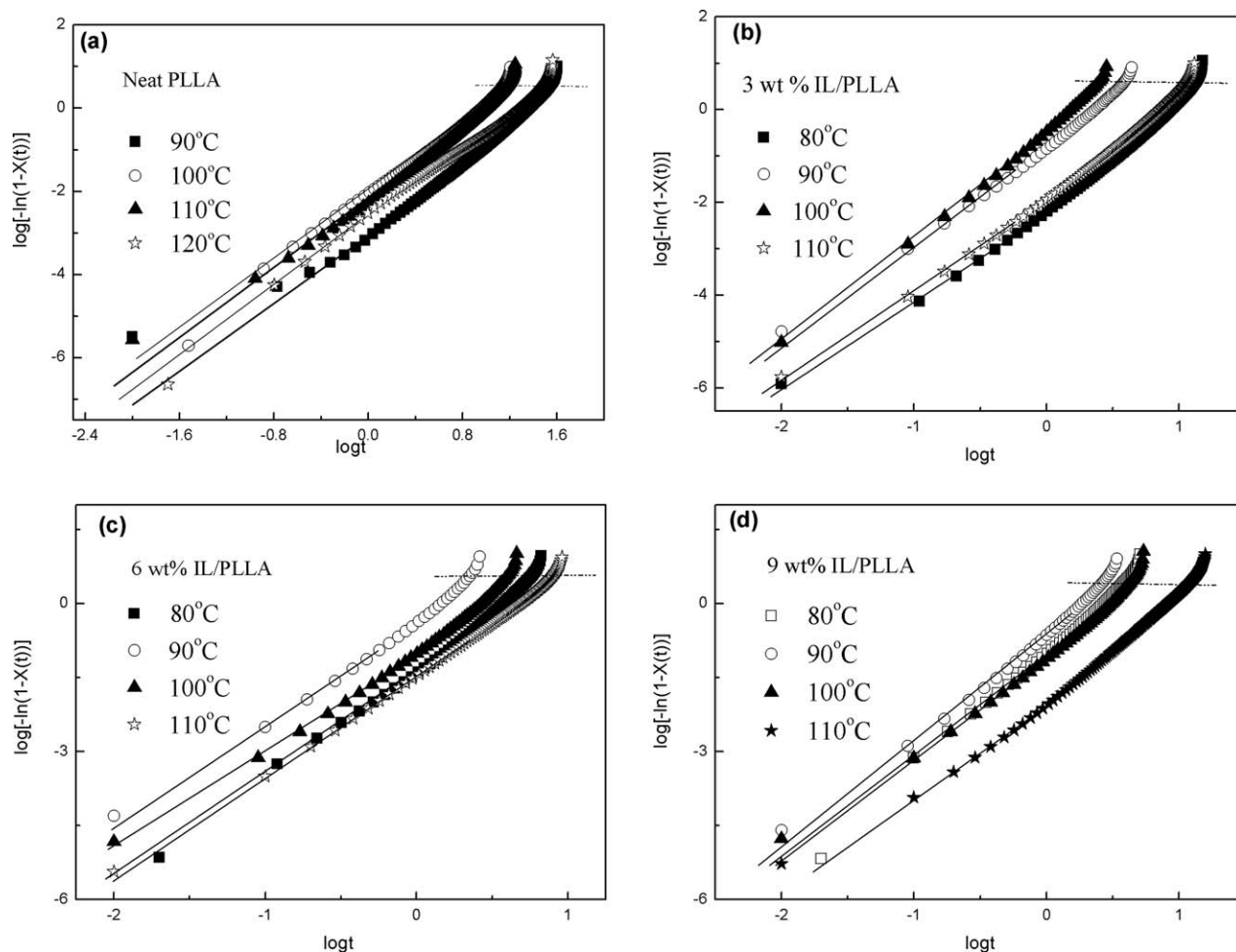


Figure 6. Avrami plots for (a) Neat PLLA; (b) 3 wt % IL/PLLA; (c) 6 wt % IL/PLLA; (d) 9 wt % IL/PLLA.

crystallization rate and crystallization ability of PLLA matrix were obviously improved due to the enhancement in PLLA segment mobility in the presence of IL.

Figure 7 shows the crystallization temperature (T_c) and component dependence of $t_{1/2}$ for neat PLLA and IL/PLLA samples. In this paper, it needs to be pointed that the time to reach the maximum crystallization degree at T_c of 80°C for neat PLLA exceeded 90 min, resulting in that the corresponding DSC exothermic peak was too weak to distinguish. Therefore, the data and plots on isothermal crystallization at T_c of 80°C for neat PLLA could not be presented.

As shown in Figure 7, it is clear that the plots of $t_{1/2}$ versus T_c is a typical ordinal rate curve with “U” type for neat PLLA.^{26–28} When T_c reached to 90°C, it is found from Figure 7 that the value of $t_{1/2}$ for neat PLLA was 19.9 min. With increasing T_c , $t_{1/2}$ became shorter and showed a minimum value of 7.9 min at 100°C. However, as T_c exceeded 110°C, the value of $t_{1/2}$ began to increase obviously.

The above result can be explained by the relation between overall crystallization rate and athletic ability of chains, as shown in Figure 8. It is well-known that the crystallization process of

semicrystalline polymers includes nucleation and crystalline growth. Therefore, the nucleation rate and the growth rate combine to dominate the overall crystallization rate. When isothermal crystallization process happens at lower temperature, the crystalline growth is restrained due to low mobility of chain segments, resulting in a slow overall crystallization rate. With the increase of T_c , the mobility of chain segments is enhanced, and the nucleating rate and crystalline growth rate are comparable. As a result, the overall crystallization rate increases largely and reaches a maximum value at an optimum temperature. However, as T_c is too high, the overall crystallization rate would decrease because the supercooling degree decreases and the excessive chain activity restricts the formation of nucleus.

As shown in Figure 7, the plots of $t_{1/2}$ versus T_c for IL/PLLA blends also are ordinal rate curves with “U” type similar with that of neat PLLA. However, it is obvious that the optimum temperature shift down with the addition of IL. These shifts mean that the maximum crystallization rate and the minimum $t_{1/2}$ for IL/PLLA samples would happen at lower temperature compared with neat PLLA. It is evident that the existence of IL can enhance the mobility of PLLA segments, leading to an

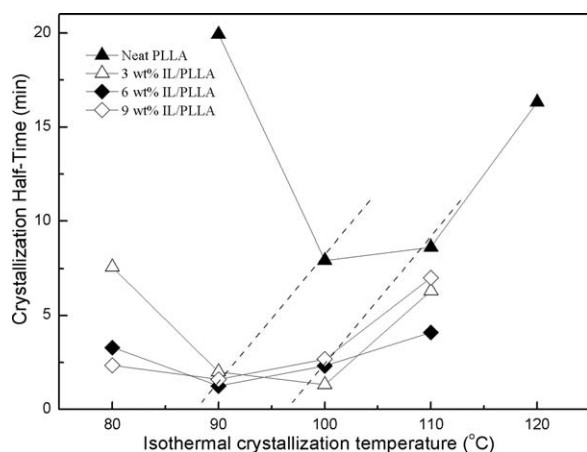
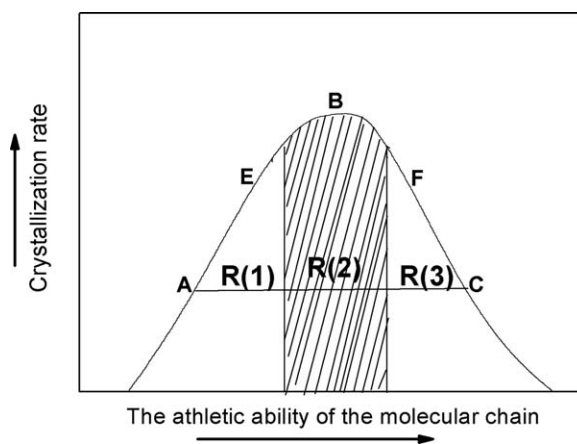
Table II. Crystallization Kinetic Parameters of Neat PLLA and IL/PLLA Samples

PLA blends	T_c (°C)	n	$\log K$	$t_{1/2}$ (min)
Neat PLLA	90	2.7	-3.67	19.9
	100	2.6	-2.48	7.9
	110	2.6	-2.62	8.6
	120	2.4	-3.07	16.3
3 wt % IL/PLLA	80	2.8	-2.62	7.6
	90	2.5	-0.91	2.0
	100	2.7	-0.49	1.3
6 wt % IL/PLLA	110	2.8	-2.24	6.3
	80	2.8	-1.64	3.3
	90	2.6	-0.41	1.3
9 wt % IL/PLLA	100	2.7	-1.17	2.3
	110	2.3	-1.54	4.1
	80	2.6	-1.14	2.4
9 wt % IL/PLLA	90	2.5	-0.67	1.6
	100	2.7	-1.30	2.7
	110	2.4	-2.17	7.0

increase in overall crystallization rate of PLLA even at a lower temperature.

To further understand the combined effect of nucleation and crystal growth on the crystallization rate of IL/PLLA samples, spherulitic morphology of neat PLLA and 3 wt % IL/PLLA blend isothermally crystallized in the temperature range of 80–120°C for 3 min were obtained using a polarized optical microscope (POM) and presented in Figure 9, respectively.

As shown in Figure 9(a), when neat PLLA was isothermally crystallized at the lower temperature ($T_c = 90^\circ\text{C}$) for 3 min, some spherulites were forming in PLLA matrix. However, the growth of these spherulites was stunted because the lower crystallization temperature lowered the mobility of PLLA segments. With increasing T_c to 100 and 110°C, as shown in Figure 9(b,c), respectively, the formed spherulites are small and appear

**Figure 7.** Plots of crystallization half-time as a function of isothermal crystallization temperature for IL/PLLA samples.**Figure 8.** The relation between overall crystallization rate and athletic ability of macromolecular segments.

in large quantity, indicating that the crystallization rate of PLLA is higher at the temperature range of 100–110°C. The extinction pattern is therefore barely recognizable due to high nuclei density. When T_c increases to 120°C, some spherulites with extinction pattern are visible in Figure 9(d). Although these spherulites' size increases largely, the nucleation density significantly decreases. It is obvious that the overall crystallization rate is relatively low as PLLA melt is isothermal crystallized at 120°C. It is because that the overall crystallization rate mainly depends on two factors before the growing spherulites impinge with each other: one is the density of the nuclei, another is the growth rate of spherulite. Generally speaking, the high crystallization temperature can accelerate the growth of each spherulite, yet largely decrease the density of the crystal nuclei. As a result, the overall crystallization rate decreased when T_c increased to 120°C, although some large spherulites with extinction cross formed in PLLA matrix. It can be confirmed from Figure 9(a–d) that the optimum crystallization temperature range for neat PLLA is 100–110°C that is consistent with DSC enthalpy measurements.

Figure 9(e–h) show the POM pictures of 3% IL/PLLA isothermally crystallized at 80, 90, 100, and 110°C for 3 min, respectively. Compared with neat PLLA isothermally crystallized at 90°C for 3 min [Figure 9(a)], it is worth mentioning that much more spherulites appear with a small size for 3% IL/PLLA isothermally crystallized at 80°C for 3 min, as shown in Figure 9(e). It indicates that the plasticizing effect of IL can increase the nuclei density and accelerate the growth of spherulites in a lower temperature. With increasing T_c to 90 and 100°C, as shown in Figure 9(f,g), respectively, the formed spherulites appear in large quantity, and become larger in size, indicating that the crystallization rate of PLLA is higher at the temperature range of 90–100°C. Interestingly, when T_c increases to 110°C, there is only a small quantity of large spherulites with extinction pattern formed in PLLA matrix, indicating that the crystallization rate of 3% IL/PLLA sample obviously decreases at 110°C.

According to the results of POM and DSC, it is confirmed that the introduction of IL can increase the nuclei density and accelerate the growth rate of spherulites especially at the lower temperatures

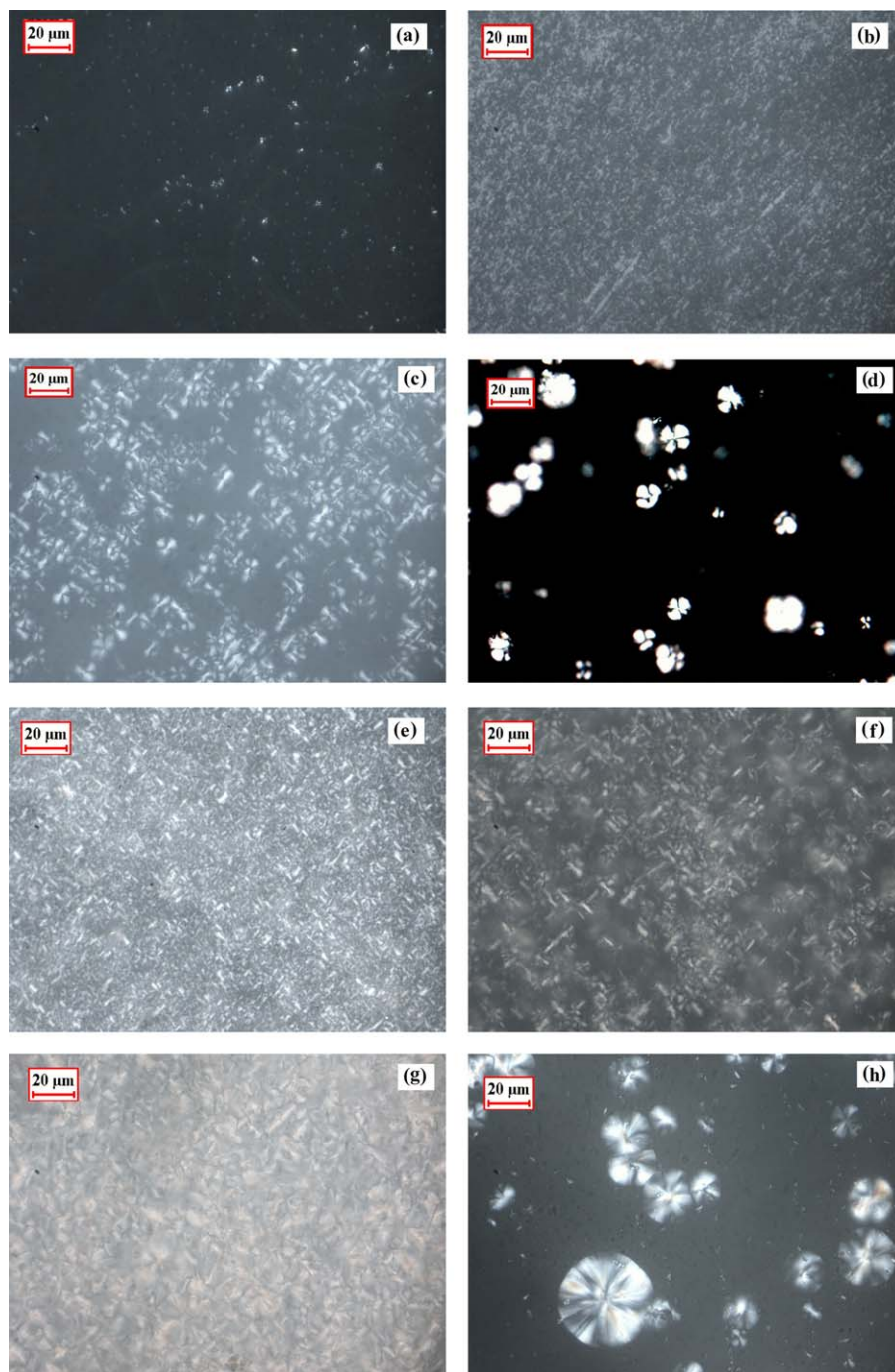


Figure 9. Polarizing optical micrographs of neat PLLA and 3 wt % IL/PLLA samples isothermally crystallized at various T_c : (a) Neat PLLA, 90°C; (b) Neat PLLA, 100°C; (c) Neat PLLA, 110°C; (d) Neat PLLA, 120°C; (e) 3 wt % IL/PLLA, 80°C; (f) 3 wt % IL/PLLA, 90°C; (g) 3 wt % IL/PLLA, 100°C; (h) 3 wt % IL/PLLA, 110°C. (All samples were isothermally crystallized for 3 minutes.) [Color figure can be viewed in the online issue, which is available at wileyonlinelibrary.com.]

due to its plasticizing effect. Actually, at the high temperature (i.e., 110°C), the motion ability of PLLA segments is enhanced too strong by IL and the nucleation is obviously restrained, that leads to a few of large spherulites with extinction cross formed at a slower overall crystallization rate. Moreover, with the addition of 3% IL, the optimum crystallization temperature range shifts down to 90–100°C from 100–110°C for neat PLLA.

To observe the morphologies of spherulites which were fully crystallized, Figure 10(a,b) shows the POM pictures of PLLA isothermally crystallized at 90 and 120°C for 30 min, respectively. It can be found that the spherulites fully grew until these spherulites impinged with each other. Because the nucleation density decreases with the increase of crystallization temperature, the spherulite's size obviously increases. The POM pictures

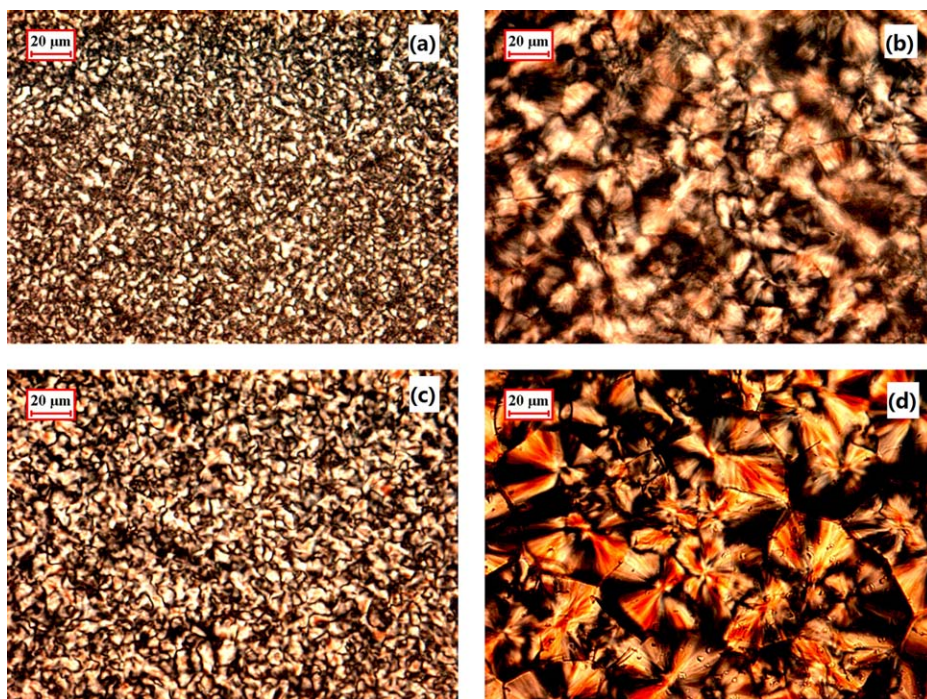


Figure 10. Polarizing optical micrographs of neat PLLA and 3 wt % IL/PLLA samples isothermally crystallized at various T_c : (a) Neat PLLA, 90°C; (b) Neat PLLA, 120°C; (c) 3 wt % IL/PLLA, 80°C; (d) 3 wt % IL/PLLA, 110°C. [All samples were isothermally crystallized for 30 minutes.] [Color figure can be viewed in the online issue, which is available at wileyonlinelibrary.com.]

of 3% IL/PLLA samples isothermally crystallized at 80 and 110°C for 30 min are also presented in Figure 10(c,d), respectively. And a similar temperature dependence of the spherulitic morphology is found from the POM pictures of 3% IL/PLLA blends. Compared with that of neat PLLA isothermally crystallized at 120°C for 30 min, the spherulite's size of 3% IL/PLLA is even larger when the blend has been isothermally crystallized at 110°C for 30 min. It is apparent that the plasticizing effect of IL can improve the growth of PLLA spherulites even in a relatively low temperature.

Moreover, it is worthy noted that the relation of IL content and $t_{1/2}$ at different T_c . It was found that the value of $t_{1/2}$ reduced with increasing IL content at lower T_c (80°C). When T_c increased to a temperature range from 90 to 100°C, the discrepancy between the values of $t_{1/2}$ for PLLA samples with various IL content is insignificant. However, as T_c increased to 110°C, $t_{1/2}$ decreased from 6.3 min for 3 wt % IL/PLLA blend to a minimum value of 4.1 min for 6 wt % IL/PLLA blend. And then, with IL content increasing to 9 wt %, $t_{1/2}$ increased to 7.0 min again.

The inconsistent trends of $t_{1/2}$ versus IL content at different T_c maybe attributed to the following factors: the nucleation density and the degree of supercooling of PLLA. When isothermal crystallization was performed at 80°C, the higher supercooling degree could make the matrix of IL/PLLA blends produce enough nuclei for crystal growth. When IL content increased from 3 wt % to 9 wt %, the mobility of chains gradually increased, which is helpful to accelerate the crystal growth and decrease the value of $t_{1/2}$. However, when the isothermal crystal-

lization happened at higher temperature (110°C), the lower supercooling degree and the presence of excess IL might show a negative effect on the formation of nuclei because the mobility of PLLA chains became too strong to form enough nuclei, which would lead to an obvious increase of $t_{1/2}$ for all IL/PLLA samples. In fact, in the lower IL content as shown in Figure 7, when IL content increased from 3 wt % to 6 wt %, it was found that $t_{1/2}$ decrease from 6.3 min for 3 wt % IL/PLLA to 4.1 min for 6 wt % IL/PLLA isothermally crystallized at 110°C. It shows that the plasticizing effect of IL on the crystallization rate of PLLA still had a positive effect in some way. However, when IL content exceed 6 wt %, the negative effect of IL on the nucleation of PLLA matrix became dominant, which caused an obvious increase of $t_{1/2}$ for PLLA blends isothermally crystallized at 110°C. The above result is similar with isothermal crystallization behavior of plasticized PLLA with triphenyl phosphate reported by Xiao et al.²⁵

As shown as Table II, compared with $t_{1/2}$ of IL/PLLA blends, the logarithm of crystallization rate constant (k) shows a similar dependence on IL content and T_c .

WXR D Analysis

In order to get further information about the crystal structure of neat PLLA and IL/PLLA samples, WXR D was used to check the crystalline nature. Figure 11 shows the WXR D patterns of neat PLLA, 3 wt % IL/PLLA and 6 wt % IL/PLLA samples, which had been fully isothermally crystallized at T_c of 100°C. When neat PLLA melt was isothermally crystallized at 100°C for 20 min, there were four peaks observed on its WXR D pattern, as shown in Figure 11. The peaks at $2\Theta = 14.9^\circ$, 16.8° ,

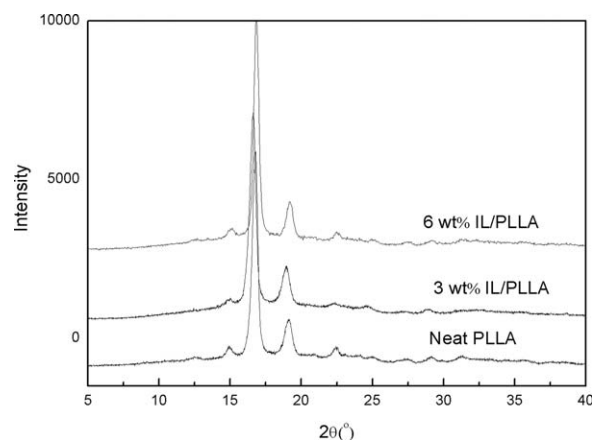


Figure 11. WAXRD patterns of crystallized neat PLLA, 3 wt %IL/PLLA and 6 wt %IL/PLLA samples.

19.0°, and 22.4° correspond, respectively, to the reflections of (010), (200) or (110), (203), and (015) planes for PLLA crystal. It can be confirmed that the obtained crystal form of neat PLLA is ascribed to the α -form.^{29,30} When IL/PLLA melts were isothermally crystallized at 100°C for 20 min, the obtained WAXRD patterns were same with that of crystallized PLLA, which indicated that the incorporation of IL could not obviously change the crystal structure of PLLA.

CONCLUSIONS

In this article, the crystallization behavior and isothermal crystallization kinetics of neat PLLA and PLLA blended with the IL, [BMIM](C₄H₉O)₂PO₂, were researched in detail by DSC, POM, and WAXRD.

The DSC results show that T_g of PLLA decreased largely with the increase of IL content due to the plasticizing effect of IL. In addition, it is found that the cold crystallization ability of PLLA was improved obviously with the addition of IL.

The isothermal crystallization kinetics of neat PLLA and IL/PLLA blends were also analyzed by DSC and described by Avrami equation. The Avrami exponent n for neat PLLA and plasticized PLLA were almost in the range of 2.5–3.0.

The overall isothermal crystallization rate of PLLA was influenced apparently by T_c and IL content. It is found that the plots of $t_{1/2}$ versus T_c are typical ordinal rate curves with “U” type for neat PLLA and plasticized PLLA. Neat PLLA had a relatively slow crystallization rate and the minimum $t_{1/2}$ was 7.9 min at the optimum temperature around 100°C. With the incorporation of IL, the $t_{1/2}$ showed a significant decrease. And the minimum $t_{1/2}$ reduced below 2min compared with the minimum $t_{1/2}$ of 7.9 min for neat PLLA. It can be found also that the optimum temperature shifted down with the introduction of IL. The shift means that the minimum $t_{1/2}$ for IL/PLLA blends would happen at a lower temperature compared with neat PLLA. It is evident that the existence of IL enhanced the mobility of PLLA segments, leading to an increase in overall crystallization rate for PLLA matrix at lower temperature. The dependences of $t_{1/2}$ on crystallization temperature and IL content were also confirmed by POM observation.

WAXRD patterns indicate that neat PLLA and its blends containing various IL contents isothermally crystallized at 100°C all formed the α -form crystal.

ACKNOWLEDGMENTS

The authors gratefully acknowledge support from Hainan University of 211 Project, Hainan University graduate-student joint training project in the discipline of materials science and engineering, and Analytical and Testing Center of Hainan University. They also thank the support from National Science Foundation of China (grant number: 51263007) and Youth science fund of Hainan University (grant number: qnjj1232).

REFERENCES

- Huddleston, J. G.; Visser, A. E.; Reichert, W. M.; Willauer, H. D.; Broker, G. A.; Rogers, R. D. *Green Chem.* **2001**, *3*, 156.
- Hallett, J. P.; Welton, T. *Chem. Rev.* **2011**, *111*, 3508.
- Lovelock, K. R. J.; Villar-Garcia, I. J.; Maier, F.; Steinrück, H.-P.; Licence, P. *Chem. Rev.* **2010**, *110*, 5158.
- Pandey, S. *Anal. Chim. Acta* **2006**, *556*, 38.
- Scott, M. P.; Rahman, M.; Brazel, C. S. *Eur. Polym. J.* **2003**, *39*, 1947.
- Rahman, M.; Brazel, C. S. *Polym. Degrad. Stab.* **2006**, *91*, 3371.
- Dias, A. M. A.; Marceneiro, S.; Braga, M. E. M.; Coelho, J. F. J.; Ferreira, A. G. M.; Simões, P. N.; Veiga, H. I. M.; Tomé, L. C.; Marrucho, I. M.; Esperança, J. M. S. S.; Matias, A. A.; Duarte, C. M. M.; Rebelo, L. P. N.; de Sousa, H. C. *Acta Biomater.* **2012**, *8*, 1366.
- Li, S.; Dang, X. *Chin. Polym. Bull.* **2010**, *11*, 76.
- Li, Y.; Wang, G.; Ye, J.; Li, Y. *Chin. Polyurethane Ind.* **2012**, *27*, 5.
- Lim, L. T.; Auras, R.; Rubino, M. *Prog. Polym. Sci.* **2008**, *33*, 820.
- Martin, O.; Averous, L. *Polymer* **2001**, *42*, 6209.
- Hu, Y.; Hu, Y. S.; Topolkarayev, V.; Hiltner, A.; Baer, E. *Polymer* **2003**, *44*, 5711.
- Kulinski, Z.; Piorkowska, E.; Gadzinowska, K.; Stasiak, M. *Biomacromolecules* **2006**, *7*, 2128.
- Ljungberg, N.; Wesslen, B. *J. Appl. Polym. Sci.* **2002**, *86*, 1227.
- Ljungberg, N.; Wesslen, B. *Biomacromolecules* **2005**, *6*, 1789.
- Ljungberg, N.; Andersson, T.; Wesslen, B. *J. Appl. Polym. Sci.* **2003**, *88*, 3239.
- Chen, B. K.; Wu, T.-Y.; Chang, Y.-M.; Chen, A. F. *Chem. Eng. J.* **2013**, *215*, 886.
- Park, K. I.; Xanthos, M. In Proc. 65th Ann. Tech. Conf. Soc. Plast. Eng.; **2007**; Vol. 53, p 2675.
- Park, K.; Ha, J. U.; Xanthos, M. *Polym. Eng. Sci.* **2010**, *50*, 1105.
- Seo, Y.; Kim, J.; Kim, K. U.; Kim, Y. C. *Polymer* **2000**, *41*, 2639.

21. Weng, W. G.; Chen, G. H.; Wu, D. *J. Polymer* **2003**, *44*, 8119.
22. Yu, J.; He, J. *Polymer* **2000**, *41*, 891.
23. Xiao, H.; Yang, L.; Ren, X.; Jiang, T.; Yeh, J.-T. *Polym. Compos.* **2010**, *31*, 2057.
24. Xiao, H.; Lu, W.; Yeh, J.-T. *J. Appl. Polym. Sci.* **2009**, *113*, 112.
25. Xiao, H.; Liu, F.; Jiang, T.; Yeh, J.-T. *J. Appl. Polym. Sci.* **2010**, *117*, 2980.
26. Nama, J. Y.; Okamoto, M.; Okamoto, H.; Nakanob, M.; Usukib, A.; Matsudac, M. *Polymer* **2006**, *47*, 1340.
27. Cai, Y.; Yan, S.; Yin, J.; Fan, Y.; Chen, X. *J. Appl. Polym. Sci.* **2011**, *121*, 1408.
28. Li, H.; Huneault, M. A. *Polymer* **2007**, *48*, 6855.
29. Mano, J. F.; Wang, Y. M.; Viana, J. C.; Denchev, Z.; Oliveira, M. J. *J. Macromol. Mater. Eng.* **2004**, *289*, 910.
30. Sarasua, J. R.; Rodriguez, N. L.; Arraiza, A. L.; Meaurio, E. *Macromolecules* **2005**, *38*, 8362.